




## Synchronization in Functional Networks of the Human Brain

Philipp Hövel<sup>1,2,3</sup>  · Aline Viol<sup>2,3</sup> · Philipp Loske<sup>2,4</sup> · Leon Merfort<sup>2</sup> · Vesna Vuksanović<sup>4</sup>

Received: 30 September 2017 / Accepted: 8 October 2018 / Published online: 25 October 2018  
© Springer Science+Business Media, LLC, part of Springer Nature 2018

### Abstract

Understanding the relationship between structural and functional organization represents one of the most important challenges in neuroscience. An increasing amount of studies show that this organization can be better understood by considering the brain as an interactive complex network. This approach has inspired a large number of computational models that combine experimental data with numerical simulations of brain interactions. In this paper, we present a summary of a data-driven computational model of synchronization between distant cortical areas that share a large number of overlapping neighboring (anatomical) connections. Such connections are derived from *in vivo* measures of brain connectivity using diffusion-weighted magnetic resonance imaging and are additionally informed by the presence of significant resting-state functionally correlated links between the areas involved. The dynamical processes of brain regions are simulated by a combination of coupled oscillator systems and a hemodynamic response model. The coupled oscillatory systems are represented by the Kuramoto phase oscillators, thus modeling phase synchrony between regional activities. The focus of this modeling approach is to characterize topological properties of functional brain correlation related to synchronization of the regional neural activity. The proposed model is able to reproduce remote synchronization between brain regions reaching reasonable agreement with the experimental functional connectivities. We show that the best agreement between model and experimental data is reached for dynamical states that exhibit a balance of synchrony and variations in synchrony providing the integration of activity between distant brain regions.

**Keywords** Nonlinear dynamics · Synchronization · Brain connectivity · Kuramoto phase oscillator · Neural activity

**Mathematics Subject Classification** 92B25 · 34C15 · 92C42

---

Communicated by Paul Newton.

---

Philipp Hövel and Vesna Vuksanović have contributed equally to this work.

---

Extended author information available on the last page of the article

## 1 Introduction

Decoding the fundamental mechanisms underlying large-scale brain integration is one of the major challenges of neuroscience. A dominant hypothesis states that phase synchronization plays an important role for the integration of the neural activities between distant sites of the brain. The interaction among distributed brain regions through phase synchronization may form the basis for cognitive processing (Womelsdorf et al. 2007; Uhlhaas et al. 2009; Bola and Sabel 2015). An increasing number of literature aims to establish a framework of models designed to deal with this issue by means of shaping patterns of the large-scale functional connectivity map (Honey et al. 2009; Deco et al. 2011; Muldoon et al. 2016; Hutchings et al. 2015; Sanz-Leon et al. 2015).

In this paper, we discuss neural synchronization using simple concepts of oscillators' dynamics (Strogatz 2000). To this purpose, we review a data-driven approach that uses a network of Kuramoto models to simulate phase synchrony in the brain at rest (Vuksanović and Hövel 2014, 2015, 2016). This is one of the models that aim to recover the interplay between brain structural and functional connectivity from the perspective of coupled oscillatory processes (Cabral et al. 2011, 2014; Bressler and Menon 2010; Breakspear et al. 2010). This model shows that remote synchronization observed in the brain at rest may be sustained by the shape of structural connectivity and simple dynamical rules.

There is evidence that brain integrative functions cannot be fully predicted from the anatomical structure (Honey et al. 2009; Hutchings et al. 2015). Subsequently, one can argue that the dynamics of information on top of structural connections enables the communication between segregated brain areas. Kuramoto phase oscillator models have been used to explore fundamental mechanisms underlying the nature of this communication. The basic idea is to incorporate topological properties of the large-scale brain connectivity in the coupling structure of the model. These properties are usually derived from white matter tractography. The model that we here present also takes into account the functional connectivity map and transmission delays based on realistic distances to help to focus on connections relevant for the brain state under consideration.

Within this framework, dynamical models of the resting brain based on the Kuramoto phase oscillators have been able to shed light on how (i) the resting-state brain activity emerges from a sufficient degree of noise and time delays (Cabral et al. 2011, 2014), (ii) relay-like interactions between distant brain areas emerge from modular network structures (Vuksanović and Hövel 2014), and (iii) the anatomical hubs in the brain synchronize their activity (Wildie and Shanahan 2012). A similar approach can be utilized to study pathological states due to the epilepsy (Hutchings et al. 2015), stroke (Vása et al. 2015), or schizophrenia (Cabral et al. 2013). An additional common feature of these models is the presence of variations in network synchrony, which is indicative of network metastability. This dynamical property allows for flexible changes of the network synchrony, i.e., partial and time-varying synchronization of neural activity across regions. These partial synchronization patterns in neural networks induce fluctuations at the level of synchrony of sub-networks leading to correlated fluctuations in low-frequency activity present in functional mag-

netic resonance imaging (fMRI) time series (Cabral et al. 2011; Wildie and Shanahan 2012; Shanahan 2010).

This paper is organized as follows: In Sect. 2, we first introduce the concept of brain networks, which can be studied using methods from graph theory. We then continue by describing principles of nonlinear dynamics behind synchronization models and their application on neural dynamics (Sect. 3). In Sect. 4, we investigate the role that synchrony and its variations play in brain activity based on simulated neural/blood-oxygen-level-dependent time series. We also provide new findings that combine different approaches used in previous studies. We conclude in Sect. 5 with a brief summary, consider model limitations, and suggest further studies.

## 2 Brain Networks and Neuroimaging Data

The brain is a complex dynamical system characterized by nonlinear interactions and emergent behaviors. This description—today nearly a consensus among neuroscientists—contrasts the approach of brain functional specialization, a concept widespread until the early twentieth century (Kanwisher 2010). A common basis of both viewpoints is the hypothesis that every mental state is connected to a physical brain state. This hypothesis is known as a *neural correlate* (Schall 2004). The functional specialization approach has triggered considerable contributions to neuroscience. Nevertheless, it faces serious limitations, mainly when employed to investigate high-level cognitive functions. On the other hand, the complex system approach has been very promising for such investigations. In short, the focus from the first to the latter approach has been shifted from where to how cognitive functions take place in the brain (Sporns 2013).

The popularization of the idea of the brain as a complex dynamical system was especially promoted by the recent development of noninvasive imaging technologies that were able to record the time-dependent activity in the human brain as a whole (Haynes and Rees 2006). Among those technologies, functional magnetic resonance imaging (fMRI) played a particularly important role. Roughly speaking, the data recorded via those functional neuroimaging techniques consist of temporal series associated with linear and nonlinear functional relationships between brain regions and are understood as a proxy for neural activity. These series are recorded from collective signals of neural populations that form synchronized local circuits. The current challenge is to unveil the rules behind global brain activity and how they are connected to the range of cognitive states.

### 2.1 Graph Theory and Brain Connectivity Maps

Graph theory or network science is a novel way to study topology of the structural and functional organization of the brain which consists of describing it in terms of nodes (brain regions) and edges (the structural connections or functional relationships). Before we discuss how to define brain connectivity using graph theoretical concepts, it

is important to clarify the distinction between two different types of large-scale brain connectivity frequently mentioned in the literature.

The *anatomical connectivity* map is the map of structural connections between brain regions (Sporns et al. 2005). This network is stable on shorter timescales, but it may change over larger times due to neuronal plasticity (Sporns 2013). The classical way to map structural connectivity is tracing neuronal paths by means of invasive and postmortem methods (Felleman and Van Essen 1991). Due to this fact, it cannot be used to create a large data set of the human brain. Alternatives come with the advance of neuroimaging techniques, such as diffusion-weighted magnetic resonance imaging (DW-MRI), where anatomical fibers may be inferred by means of statistical models. Such methods allow in vivo tractography of white matter fibers. See Ciccarelli et al. (2008), Clayden (2013) and Jbabdi et al. (2015) for details about structural connectivity and how to acquire it from the human brain. Figure 1 depicts a schematic illustration of the workflow to extract a brain graph from imaging data. In short, the adjacency matrix is obtained from the anatomical connectivity probability map by thresholding, that is, only probabilities above a threshold result in a link in the brain graph.

The procedure of DW-MRI leads to probabilistic structural connectivity maps. In order to quantify the probability, with which two brain regions of interest are structurally connected, one constructs a three-dimensional trajectory of the fiber tract

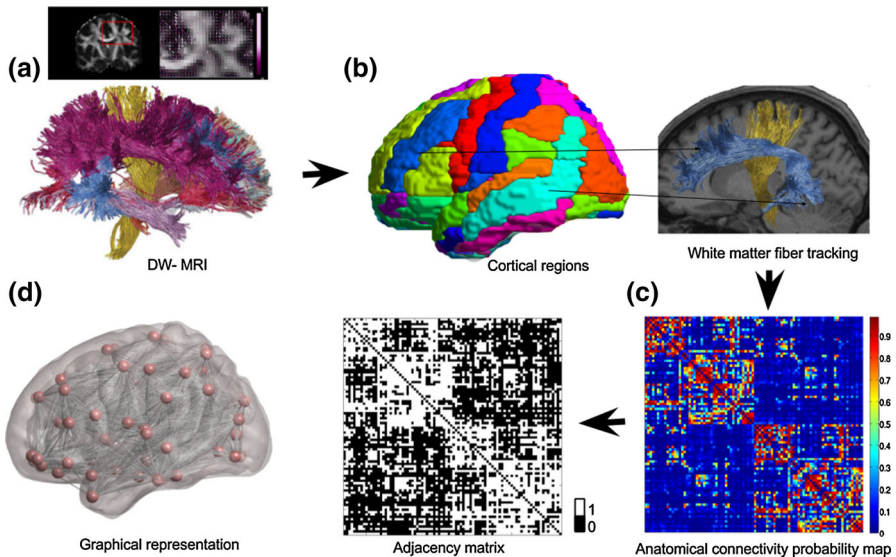


**Fig. 1** Anatomical network. **a** Diffusion-weighted magnetic resonance imaging (DW-MRI) and artistic reconstruction showing the fiber tracts. **b** Parcellation according to a cortical anatomical atlas and density of tracts between two pairs of areas. **c** Matrix of the anatomical connectivity probability of structural connections between pairs of regions. **d** Network construction: adjacency matrix obtained by thresholding and graphical representation of the corresponding structural brain network. Sources: The DW-MRI figure and its artistic reconstruction is a reproduction of Farooq et al. (2016). The brain images and network were created with the help of BrainNet Viewer (Xia et al. 2013). The data for the anatomical connectivity probability are taken from Iturria-Medina et al. (2008)

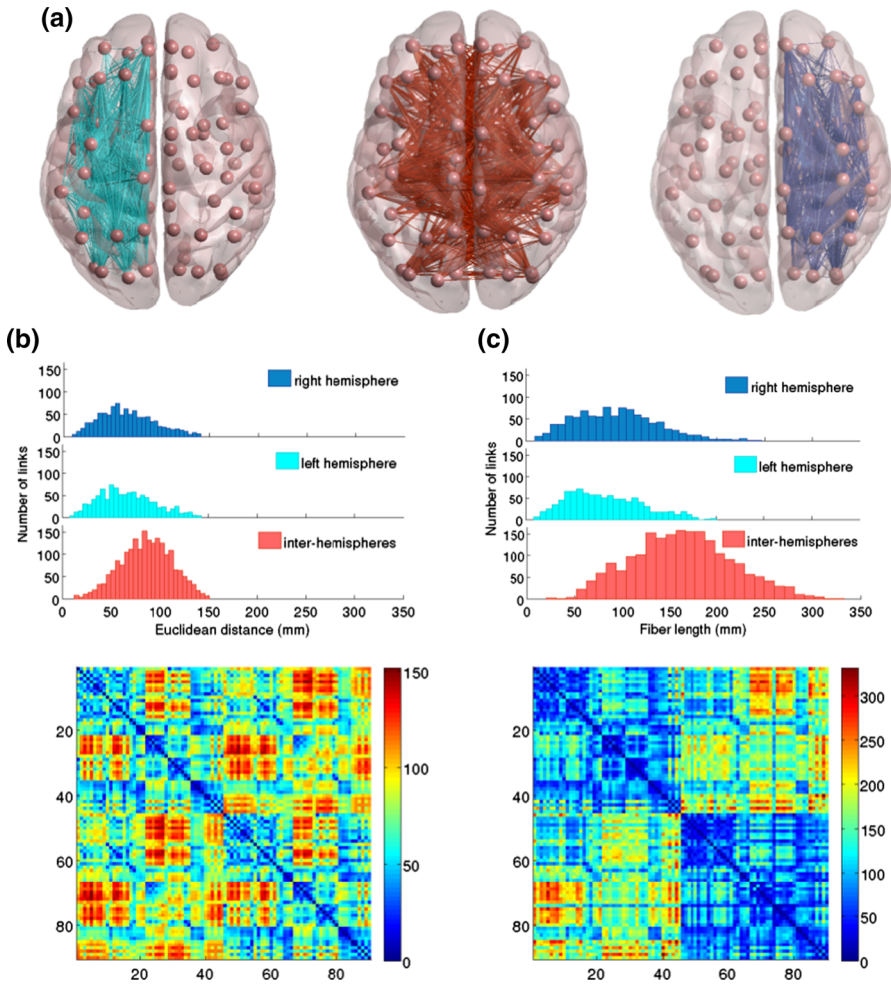


**Fig. 2** Euclidean distances and fiber lengths. **a** Representation of networks, that is, 90 brain regions according to the Automated Anatomical Labeling (AAL) parcellation (Tzourio-Mazoyer et al. 2002) as nodes connected by links in the left hemisphere, between hemispheres, and in the right hemisphere respectively. **b** Top: histograms of Euclidean distances in the right (blue), left (cyan), and between (red) hemispheres. Bottom: matrix of the Euclidean distances between pairs of cortical regions. **c** Top: histograms of the fiber lengths in the right, left, and between hemispheres. Bottom: matrix of the fiber lengths between pairs of cortical regions. The data of the fiber lengths were taken from Iturria-Medina et al. (2008). The brain networks were created with help of BrainNet Viewer (Xia et al. 2013) (Color figure online)

between the centers of those regions. This provides a gateway to measure the length of the connection. Figure 2 depicts the distribution and distance matrices of these fiber lengths in panel (c). Compared to a naive estimate based on the Euclidean distance between regions considered in the Automated Anatomical Labeling (AAL, see Tzourio-Mazoyer et al. 2002) shown in panel (b), one can see that the distributions of intra- and inter-hemispheric connections exhibit qualitatively the same shape and that

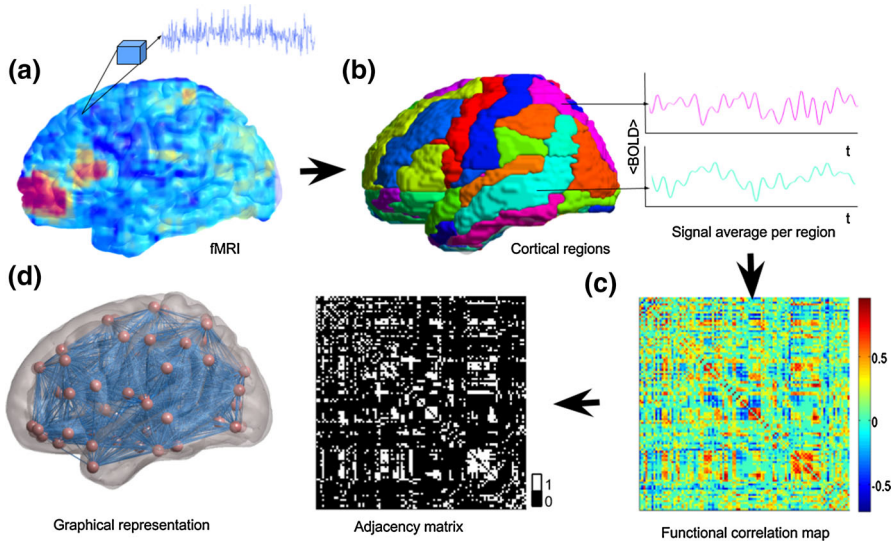


**Fig. 3** Functional network. **a** Functional magnetic resonance imaging (fMRI) and blood-oxygen-level-dependent (BOLD) signals recorded for each voxel. **b** Parcellation according to cortical anatomical atlas and the averages of the signals for two regions. **c** Functional correlation between BOLD time series for every pair of regions. **d** Network construction: the adjacency matrix obtained by thresholding and the corresponding functional brain network. The brain images and network were created with the help of BrainNet Viewer (Xia et al. 2013)

the fiber lengths stretch to larger values. As it will be explained in detail in Sect. 3.2, this distance can be used to approach transmission delays between the brain regions.

Functional relationships in the brain are usually described in the form of so-called functional connectivity maps. They map the temporal correlations between regional activities (Heeger and Ress 2002), whose modular-like organization supports resting-state networks as well as cognitive and behavioral functions. Therefore, they refer to a functional relationship irrespective of whether or not there exist anatomical connections. Functional connectivities are derived from time traces obtained by recordings of variations in the blood-oxygen-level-dependent signal (BOLD signal) due to brain activity. For a schematic depiction of the generation of functional connectivity maps, see Fig. 3. In this work, we are interested in simulating the functional connectivity based on networks obtained from neuroimaging data. In the following, we briefly describe how a functional connectivity map, or functional network, can be obtained from fMRI data using graph theory.

The fMRI data are a three-dimensional image of the brain acquired over time. At the finest spatial resolution of such an image, each *voxel* (typically of size  $1\text{--}2\text{ mm}^3$ ) gives rise to a single time series. For a large-scale analysis of the whole brain, the functional network may be defined as follows: The graph nodes represent regions of interest, usually defined by cortical regions obtained by parcellating the voxels in the fMRI measurement according to a cortical brain atlas (Tzourio-Mazoyer et al. 2002; Talairach and Tournoux 1988). Each of the resulting regions of interest, that is, nodes in the brain network, gives rise to one time series that represents the BOLD signal

in this region. Usually, this series is obtained by averaging over the respective set of voxels. Subsequently, network links are defined on the basis of a correlation between time series from each pair of regions of interest. This method yields a weighted coupled network, indicating the similarity in the activities of the respective nodes. These maps *connect* brain regions irrespective of the presence of actual anatomical links. It is worth mentioning that fMRI captures the variation in the BOLD signal; that is, it is an indirect measurement of neural activity and includes several confounders (Greve et al. 2013). Before constructing functional networks, the data undergo a number of preprocessing steps, e.g., for motion correction, to remove spurious information, and band-pass filtering to improve the signal-to-noise ratio. For further details about data preprocessing, see Vuksanović and Hövel (2014), Power et al. (2014), Kruggel et al. (1999), and Desjardins et al. (2001). For more details about networks from fMRI data, see Rubinov and Sporns (2010), Bullmore and Bassett (2011), Liu et al. (2008), and Onias et al. (2014).

One can describe functional networks by an adjacency matrix  $\{A_{ij}\}_{i,j=1,\dots,N}$ , in which each matrix element takes the value of unity if a pair of nodes is connected and zero otherwise. The pair of nodes is considered to be connected when the respective entry in the correlation matrix exceeds a predefined threshold value. There are different methods used to threshold the matrix and to retain only those values which are statistically significant. The value of the threshold has a direct influence on the network density (Bullmore and Bassett 2011): The higher the threshold, the lower the network density. By defining its adjacency matrix and thus selecting the network topology, it is possible to detect universal behaviors of coupled dynamical systems such as synchronization or metastability. One can also consider weighted instead of binarized matrices. The weight can be added to the model by considering some information from experimental data. For example, it can be proportional to the density of fiber tracts between the two cortical regions (Cabral et al. 2014). In the current approach, however, we aim for simplicity of the model by considering only anatomically relevant connections of higher probability. For a detailed overview of complex brain networks, see Sporns (2011).

## 2.2 Spontaneous Synchronicity and Resting-State Brain Networks

Most of the early neuroimaging analyses were designed to test the hypothesis of localized functional brain specificity. The goal was to investigate, which region in the brain is activated during a specific task. This design is rooted in neuroanatomists' concepts of the eighteenth century and was largely discussed at the end of the twentieth century (Kanwisher 2010). In fact, several experiments had supported the paradigm that specific brain regions are correlated with specific functions, especially basic sensory and motor tasks (Kanwisher 2010). However, the functional specificity started to receive relevant critical remarks. This reductionist approach could not explain high-level cognitive processes such as emotions, creativity, and consciousness.

In the middle of the 1990s, a new insight changed the focus of research and transformed prior knowledge. It was recognized that there are large-scale synchronization patterns in the spontaneous fluctuation of brain activities in the absence of external

input (Biswal et al. 1995). Non-random patterns were observed in the data scanned from subjects in the resting state, that is, lying down in the absence of tasks or attention demands. These findings were corroborated and complemented by several studies using different neuroimaging techniques (Lowe 2010). Further descriptions of these patterns, termed as *resting-state networks* (RSN), can be found in Cole et al. (2010) and van den Heuvel and Hulshoff Pol (2010). The discovery of the RSN is considered a milestone in contemporary neuroscience for different reasons. It supports the regard of the brain as a dynamical complex system. The detection of large-scale patterns for resting-state conditions reflects the existence of coordinated intrinsic dynamics. This spontaneous inter-regional synchronization indicates self-organized capability. On the one hand, it has been suggested that RSN are related to high-level brain functions such as internal mental processes and consciousness. This hypothesis is supported by studies that show variations in statistical features of RSN in altered states of consciousness (Tagliazucchi et al. 2014; Carhart-Harris et al. 2016; Viol et al. 2017) and mental disorders such as autism (Rudie et al. 2013) or schizophrenia (Rubinov et al. 2009). On the other hand, RSN have also been detected in people subjected to deep sedation (Schrouff et al. 2011), sleep (Dang-Vu et al. 2008), coma (Noirhomme et al. 2010), or even vegetative states (Huang et al. 2014). This fact could, in principle, challenge the hypothesis of RSN as a signature of consciousness. However, Barttfeld et al. show that RSN in monkey brains under deep anesthesia are more strongly correlated with the anatomical connectivity map in comparison with regular RSN in a resting state of wakefulness (Barttfeld et al. 2015). They show that in the case of loss of consciousness, the functional activity is tied to anatomical connectivity. Their study is in agreement with hypotheses made in previous theoretical works (Deco et al. 2011, 2013). Functional networks in resting states where the subject is awake are characterized by long-range synchronicity and high variability of patterns. It had been observed that an anatomically connected pair of nodes has a high probability to be functionally connected. However, functional connectivity is frequently observed between brain regions without direct structural links (Deco et al. 2011; Koch et al. 2002). The understanding of the rules that allow both long-range synchronization and flexibility of patterns on functional networks may be the key to decrypt the mechanisms behind high-level brain functions. Models using dynamical systems, e.g., oscillator models, are the most promising tools to tackle this challenge.

### 3 Brain Activity and Synchronization Models

In this section, we build a bridge between nonlinear dynamics and computational neuroscience. At first, we summarize the concept of synchronization and then develop a simple mathematical model that will be used in Sect. 4. We also briefly elaborate, how a BOLD signal can be inferred from a neural time series by means of the Balloon–Windkessel model.



### 3.1 Nonlinear Dynamics and Synchronization in the Brain

Synchronization plays an important role in various contexts including physics, biology, and beyond (Strogatz 2000; Pikovsky et al. 2001; Boccaletti et al. 2002; Mosekilde et al. 2002; Balanov et al. 2009). In neuroscience, some forms of cooperative dynamics have been associated with pathological states like migraine, Parkinson's disease, or epilepsy (Rossoni et al. 2005; Wang and Lu 2005; Hauptmann et al. 2007; Masoller et al. 2008; Wang et al. 2008, 2009; Masoller et al. 2009; Senthilkumar et al. 2009; Liang et al. 2009; Lehnert et al. 2011; Popovych et al. 2011). Besides these detrimental forms of synchrony, it is also considered a crucial mechanism for recognition, learning, and processing of neural information.

In general, neuronal systems can be described by physiological models such as the Hodgkin–Huxley equations (Hodgkin and Huxley 1952). These type of models account for many physiological details and processes. Accordingly, they offer a detailed description of a single cell. On the downside, they often consist of many equations and many parameters and their applicability on large ensembles of elements is highly questionable, which also holds for a bifurcation analysis.

On the other side of the spectrum of complexity, there are normal-form equations. These phenomenological models capture the main dynamical behavior of neurons such as the type of excitability and can be coupled together in large networks with reasonable numerical effort. In some cases like the FitzHugh–Nagumo model (FitzHugh 1961; Nagumo et al. 1962), they can be derived as low-dimensional approximations, which are better suited for a bifurcation analysis, because they contain only a few parameters and nonlinearities. The price that one has to pay is a vague—at best qualitative—correspondence to physiological quantities like membrane potential and ionic currents.

Self-organized dynamics of brain regions into functional networks often follow the underlying structural connections. There are, however, functional correlations between cortical regions that are not directly connected. Thus, the mechanisms for functional connectivity between distant cortical regions are still subject to intense research efforts. For example, indirect connections can support collective dynamical behavior on the brain network and pronounced pair-wise correlation of brain regions. If such indirect connections are involved, that is, there is no direct anatomical link between highly correlated regions, the dynamical pattern can be called *remote synchronization* (Bergner et al. 2012; Nicosia et al. 2013). The amount of synchrony depends on properties of the coupling topology such as the symmetry of interactions (Nicosia et al. 2013; Arenas et al. 2006).

### 3.2 The Kuramoto Model of Phase Oscillators

Neural activity evolves through brain networks as a dynamical process, which can be approximated by either neural fields (Jirsa and Haken 1996) or neural models (Izhikevich 2004). To simulate the dynamical behavior of such processes, one can also choose the even simpler, that is less complex, model of Kuramoto-like phase oscillators (Vuksanović and Hövel 2014, 2015; Cabral et al. 2011; Breakspear et al. 2010), which has been established as a general model for oscillatory dynamics.

The classic Kuramoto model consists of dynamical equations with one phase variable for each network node (Kuramoto 1975). The nodes are connected in an all-to-all topology and the interactions are mediated by sinusoidal functions of the phase differences of all pairs of oscillators:

$$\dot{\phi}_i = \omega_i + \frac{K}{N} \sum_{j=1}^N \sin[\phi_j(t) - \phi_i(t)], \quad i = 1, \dots, N, \quad (1)$$

where  $K$  is a global coupling strength. The parameter  $\omega_i$  denotes the natural frequency of the  $i$ th oscillator drawn from a given distribution. For reviews on the relevance and universal applicability of the Kuramoto model, see Acebrón et al. (2005) and Rodrigues et al. (2016).

In order to analyze the amount of synchrony in the network, the global order parameter, which is given by the center of mass of phase variables of each node distributed on the unit circle, has proved to be very insightful:

$$R(t) = \left| \left\langle e^{i\phi_k(t)} \right\rangle_N \right|, \quad k = 1, \dots, N, \quad (2)$$

where  $\langle \cdot \rangle_N$  denotes the average over all nodes in the network. The order parameter can easily be applied to the simulated time series of neural activity (Cabral et al. 2011; Hellyer et al. 2014; Cabral et al. 2012). Then, its temporal mean value  $\langle R(t) \rangle$  and standard deviation provide information about the level and temporal fluctuations of synchrony. The latter can be interpreted as metastability as discussed below. It is easy to see that in Eq. (2),  $R(t)$  tends to zero, if the phase variables are dispersed across phase space, that is, when they are highly desynchronized. In the opposite case, when most of oscillators have close phase variables, one obtains the limit  $R(t) \rightarrow 1$ .

In general, the number of phase variables that become locked and synchronized, depends on the coupling strength  $K$ . This quantity can be used as a control parameter to study emerging patterns of synchrony. For a given natural frequency distribution, there is a threshold or critical coupling strength  $K_c$  above which the coupled system starts to synchronize. This observation can be described as a phase transition. Results based on the global order parameter defined in Eq. (2) can be seen as a mean-field approach, that is, the simplest case of isotropic interaction.

To study neurobiological systems, it is necessary to consider inhomogeneities of the coupling topology connected to a variety of different complex networks. In addition, one can investigate the influence of time delay in the coupling term. Then, Eq. (1) can be extended as follows

$$\dot{\phi}_i = \omega_i + C \sum_{j=1}^N A_{ij} \sin[\phi_j(t - \tau_{ij}) - \phi_i(t)], \quad i = 1, \dots, N, \quad (3)$$

where the coupling strength is denoted by  $C$ . Now, structural inhomogeneities can be accounted for by pair-wise transmission delays  $\tau_{ij}$  in the coupling term. This makes network interactions biologically more plausible (Breakspear et al. 2010, 2006) and

prevents full synchronization of the network (Nicosia et al. 2013; Keane et al. 2012). The delays are inferred from the distance  $\Delta_{ij}$  between nodes  $i$  and  $j$ :  $\tau_{ij} = \Delta_{ij}/v$  with a signal propagation velocity  $v$  in the range of 1 m/s to 20 m/s. Alternatively, one can introduce link-dependent phase offsets in the coupling term (Vuksanović and Hövel 2016). Less pronounced synchronization can be interpreted as a preferred dynamical state and an important property of the neural networks, as fully synchronized brain dynamics are never observed experimentally. From the results of models of the resting-state dynamics, for instance, it has been argued that the brain operates in so-called metastable states and never reaches full synchronization (Cabral et al. 2014; Deco and Jirsa 2012).

The network matrix  $\{A_{ij}\}$  defines the interactions between the neural processes. As elaborated in Sect. 2, one can construct this matrix using empirically derived structural connectivity: The nonzero entries of the matrix correspond to existing connections between respective brain regions. Alternatively, one could also generate an adjacency matrix based on the functional connectivity. Further details on the applied procedure, which uses a combination of anatomical and functional connectivity maps, will be discussed in Sect. 4. See also Fig. 4.

### 3.3 Inferring BOLD Signals: The Balloon–Windkessel Model

As mentioned in Sect. 2.1, functional connectivity maps are networks of brain regions that are based on a statistical dependence between fMRI time series (Bressler and Menon 2010; Biswal et al. 1995; Damoiseaux et al. 2006). The underlying time series of BOLD activity are a function of changes in cerebral blood flow, cerebral blood volume, and cerebral metabolic rate of oxygen consumption and typically exhibit significant correlations for frequencies below 0.1 Hz in the resting state (Biswal et al. 1995). In order to compare the numerically obtained neuronal activity with the empirical BOLD signal, we make use of the Balloon–Windkessel model (Friston et al. 2000), which has been established in many computational studies of the resting-state brain activity. Briefly summarized, this model considers the neuronal time series as an input signal (Seth et al. 2013) and computes the hemodynamic response, which can then be related to the BOLD signal. Since the neuronal activity and the blood response operate on different timescales of milliseconds and seconds, respectively, the Balloon–Windkessel model acts as a low-pass filter on the high-frequency neuronal signal. To allow for comparison with the experimentally measured BOLD signal, we match a simulation’s duration to the lengths of the experimental recording.

## 4 Data-Inspired Models: From Neuroimaging Information to Brain Activity Models

From a modeling perspective, the observed spatiotemporal patterns in brain activity are shaped by the complex relationship between the dynamics of individual oscillators and global synchronization (Friston and Dolan 2010). As described in Sect. 3.2, these competing dynamics can be characterized by the amount of synchrony in the

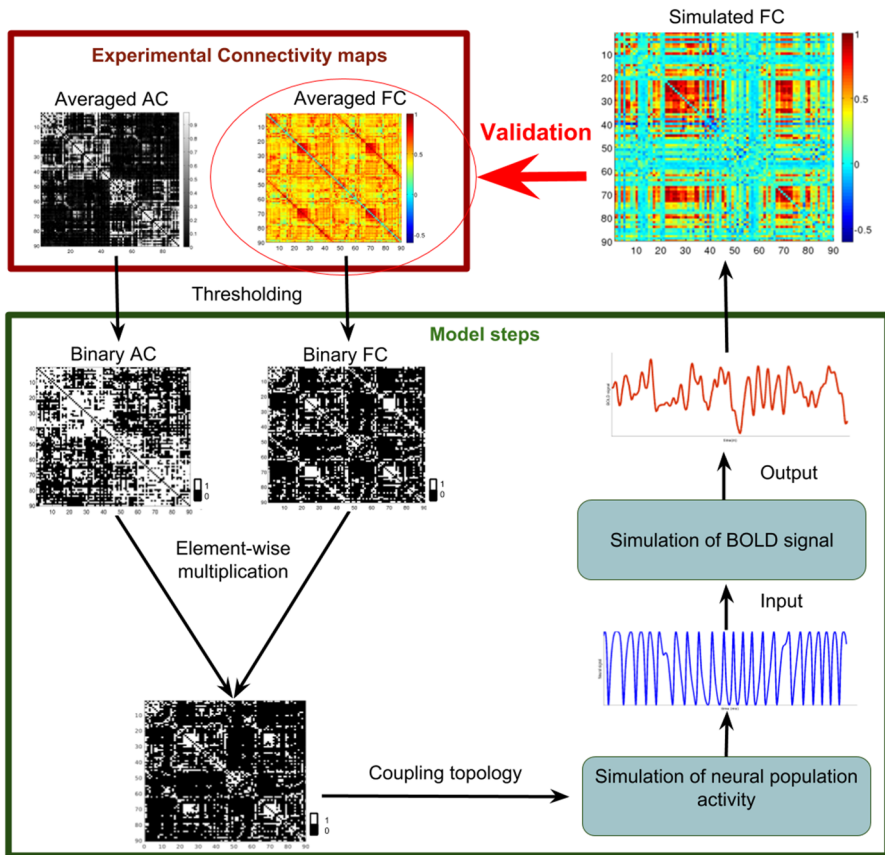


**Fig. 4** Schematic diagram of the modeling framework. Anatomical connectivity (AC) and functional connectivity (FC) maps extracted from DW-MRI and fMRI as group averages over 26 subjects, respectively, are binarized and combined to compute the adjacency matrix that provides the coupling topology in the simulations. Neural population activity is simulated and used as input to infer the simulated BOLD signal. The resulting time series of each node are correlated pair-wise leading to a simulated functional connectivity matrix, which is compared with the experimental functional connectivity map

network and its variations over time. The latter indicates dynamical metastability. It has been suggested that these variations of the network synchrony shape the patterns of coordinated activity between brain regions, thus enabling dynamical exploration of different network configurations (Cabral et al. 2014; Hellyer et al. 2014; Tognoli and Kelso 2014). Such functional network configurations are constrained by the underlying anatomical structure (Bullmore and Sporns 2009)—another key ingredient of the model.

Anatomical brain connections enter models of the brain dynamics in the form of the coupling matrix, whose elements represent actual neural paths between brain regions—network nodes—as described in Sect. 2.1. The topology of this matrix is usually static, i.e., the number of links between the nodes is preserved. Figure 4 provides a schematic diagram of the model workflow. A combination of experimental anatomical

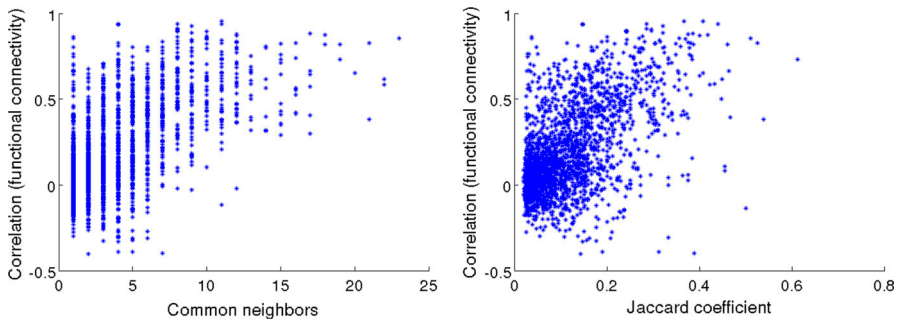


**Fig. 5** Functional connectivity between pairs of network nodes, i.e., regions of interest that are not directly connected in the considered brain graph, as a function of the number of common neighbors (left) and Jaccard coefficient (right). Parameters in the simulation of Eq. (3) with delays calculated from the fiber lengths: threshold for functional connectivity in the network generation  $r = 0.56$ , coupling strength  $C = 54$ , and signal transmission velocity  $v = 5$  m/s

and functional connectivity maps leads to an adjacency matrix that defines the interaction of the oscillators in the simulations. A link is present if it is anatomically justified and has a high probability to have functional connectivity, which is implemented as an element-wise multiplication of binarized anatomical and functional connectivity matrices. By averaging and binarizing the connectivity matrices, one can select the connections between pairs of regions with higher statistical probability, considering all subjects. Since the functional connectivity map has been derived from resting-state data, the element-wise multiplication selects those anatomical connections that directly connect brain regions that tend to be highly correlated in this condition. This step is important to evaluate the first level influence of anatomical connections in the remote synchronization of brain regions activities.

We use this approach to derive the coupling topology for our simulations as our primary aim is to reconstruct long-distance functional correlations that emerge from the underlying anatomical paths. Previous works have used this model to explore the contribution of the long-distance functional interactions—those that are not supported by direct neural paths—to the brain functional correlations in the resting-state activity (Vuksanović and Hövel 2014, 2015). These works have shown that the integration of the brain functions may arise from relay-like phase interactions between neural oscillators that share large parts of their individual network’s neighborhood. In this review, we present additional analyses based on brain dynamics that include time delays in the phase interactions between the neural oscillators, as given in Eq. (3). The time-delayed interactions are determined by the empirical length of the connections between the regions. See Fig. 2. It is worth mentioning that the time delays on the real brain may be affected by heterogeneities related to local physiology. For example, the velocity of signal transmission depends on other biological aspects such as myelination and axon thickness. The model in this paper accounts for the influence of time delay by (i) considering the heterogeneity of distances and (ii) assuming a fixed velocity.

Figure 5 shows the effect of remote synchronization. It depicts the functional connectivity for any pair of nodes  $i$  and  $j$  that do not share a direct connection according to the coupling matrix in dependence on the number of common neighbors and the

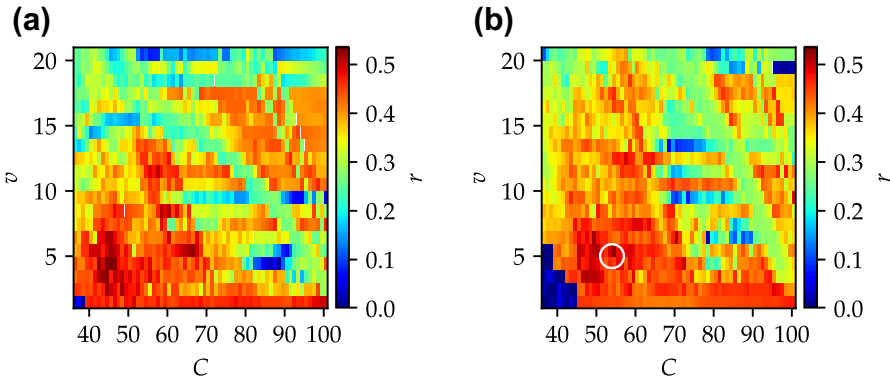


**Fig. 6** Pearson correlation coefficient between experimentally derived and simulated functional connectivity in the parameter space spanned by coupling strength  $C$  and signal transmission velocity  $v$ . The simulations are based on Eq. (3) with time delays calculated from the Euclidean distances and lengths of fiber tracks between regions of interest in panels (a) and (b), respectively. See Fig. 2 for further information on the distances. The white circle in panel (b) marks the  $(C, v)$  values used in Figs. 5 and 7 with a maximum Pearson correlation of 0.53

relative overlap of the neighborhoods  $N_i$  and  $N_j$ . The latter is quantified by the Jaccard coefficient

$$J_{ij} = \frac{|N_i \cap N_j|}{|N_i \cup N_j|}, \quad (4)$$

where  $|N_i|$  denotes the number of neighbors of node  $i$ , that is, its degree. In words,  $J_{ij}$  is the relative size of the intersection between the two node sets with respect to their union and takes values in the interval  $[0, 1]$  with the limit cases of zero and unity referring to no and perfect overlap, respectively. We observe an increase in functional connectivity as the overlap of neighborhoods becomes larger. This is in agreement with previous findings (Vuksanović and Hövel 2014, 2015).

A systematic exploration of the parameter space spanned by coupling strength  $C$  and signal transmission velocity  $v$  is depicted in Fig. 6, where the left and right panels refer to time delays in Eq. (3) according to the Euclidean distances and lengths of fiber tracks between brain network nodes, respectively. Recall that the finite velocity is the cause of delayed interactions. The color code indicates the agreement with the experimentally derived and simulated functional connectivity quantified by the Pearson correlation coefficient. Overall, the results of the two panels in Fig. 6 are qualitatively very similar. Note that a rescaling in the  $v$ -direction would lead to a quantitative agreement that could be explained by the shape of the distance distributions shown in Fig. 2. Larger velocities could compensate for the longer distances. According to our analysis, the Euclidean distance between different brain regions—with a proper scaling factor—can be used to account for finite signal transmission velocities along the neural connections. The highest Pearson correlation is found in the range of plausible transmission velocities. For weak coupling, that is, low values of  $C$ , the interaction via the network is not strong enough to trigger significant self-organized synchrony in neural activity or BOLD signals.

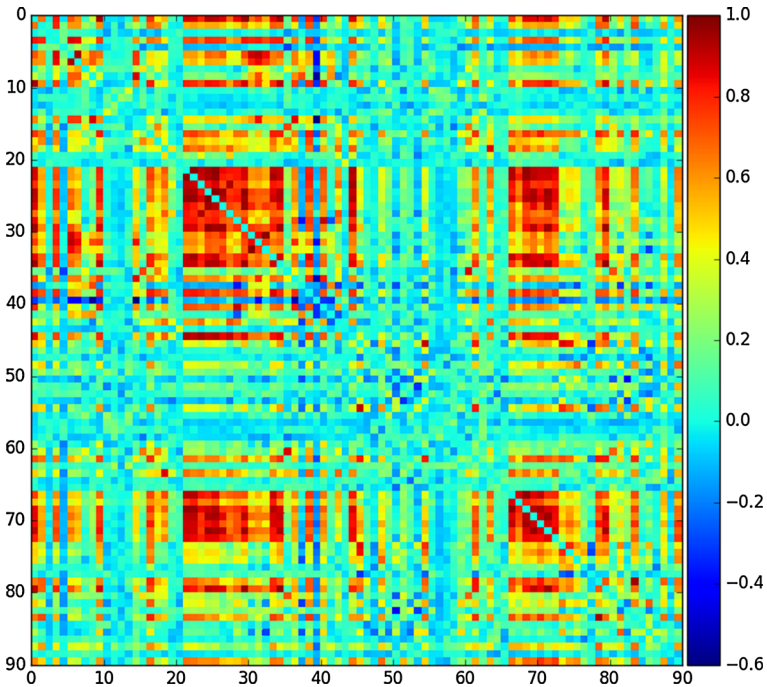


**Fig. 7** Exemplary, simulated functional connectivity based on Eq. (3) with time delays calculated from the fiber lengths between regions of interest (cf. Fig. 2). Parameters:  $C = 54$  and  $v = 5$  m/s

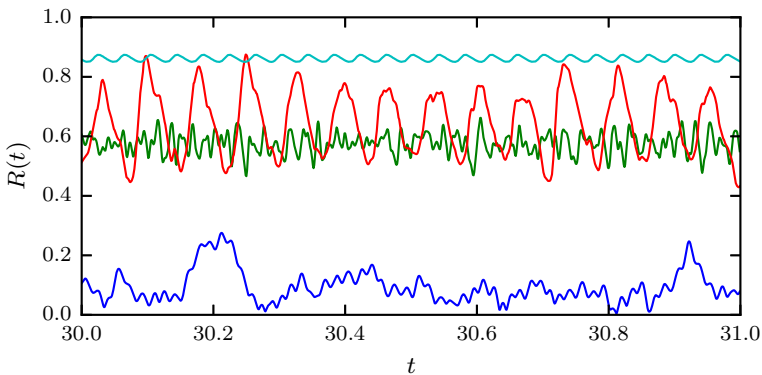


**Fig. 8** Global order parameter defined in Eq. (2) for different signal transmission velocities  $v = 0.1$  m/s (blue), 5 m/s (green), 20 m/s (red), and 100 m/s (cyan). The coupling strength is fixed at  $C = 54$  (Color figure online)

The best agreement of the simulated functional connectivity with the experimental functional connectivity is observed for  $C = 54$  and  $v = 5$  m/s. Figure 7 shows the corresponding functional connectivity matrix obtained from the simulations. One can see clusters of well-correlated nodes in the brain network.

Considering the form of the global order parameter  $R$  given by Eq. (2), the particular parameter combination choice,  $C = 54$  and  $v = 5$  m/s, is justified. The temporal

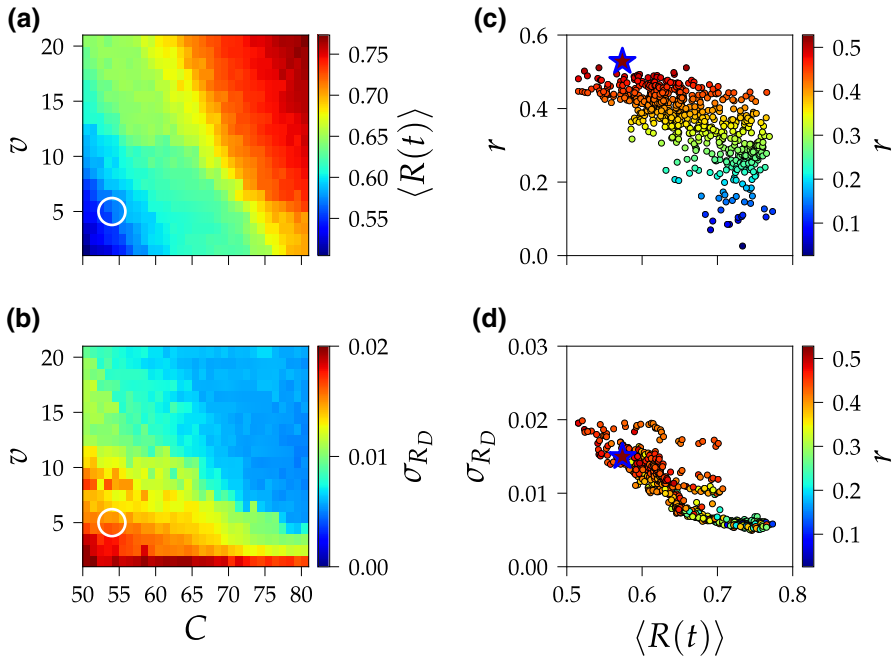


**Fig. 9** Panels (a) and (b): parameter scan of the average order parameter  $\langle R(t) \rangle$  and detrended fluctuations  $\sigma_{R_D}$  as color code in the  $(C, v)$ -plane, respectively (cf. Fig. 6). Panels (c) and (d): average order parameter  $\langle R(t) \rangle$  versus Pearson correlation coefficient  $r$  and detrended fluctuations  $\sigma_{R_D}$ , respectively. The color code refers to the Pearson correlation coefficient  $r$  between experimental and simulated functional connectivity (cf. Fig. 6). The white circles and blue star marks the values  $C = 54$  and  $v = 5$  m/s used in Figs. 5 and 7 with a maximum Pearson correlation of 0.53. The fit of the modeled functional correlations with the experimental data is best for a dynamical state that simultaneously balances synchrony and metastability (Color figure online)

average  $\langle R(t) \rangle$  of the order parameter quantifies the average amount of synchrony in the brain network and its standard deviation can be used to characterize metastability. Figure 8 depicts the time series of  $R$  for a fixed coupling strength  $C = 54$  and different velocities  $v$ . Large values of  $v$  result in an almost instantaneous coupling, for which the coupling function in Eq. (3) supports the emergence of robust synchronization. This is indicated by a high value of  $R$  that does not exhibit strong fluctuations around its mean (cyan curve,  $v = 100$  m/s). As velocities decrease, the order parameter becomes smaller, but still maintains its periodicity (red curve,  $v = 20$  m/s). In the range of plausible velocities (cf. green curve,  $v = 5$  m/s), we find a balance between synchrony and metastability, that is, a reasonable value of  $\langle R(t) \rangle$  together with seemingly random fluctuations. These observations are in agreement with our previous studies (Vuksanović and Hövel 2014, 2015).

Figure 9 shows how functional interactions—high values of the correlation coefficient  $r$  between the modeled and experimental dynamics—can be connected to a dynamical behavior that balances the synchrony  $\langle R(t) \rangle$  and the variations in synchrony  $\sigma_{R_D}$ . Figure 9a, b depicts the dependence of the average order parameter  $\langle R \rangle$  and its fluctuations  $\sigma_{R_D}$  on the coupling strength  $C$  and the transmission velocity  $v$ ,



respectively. For the fluctuations  $\sigma_{R_D}$ , we detrended the periodic behavior of  $R(t)$  (cf. Fig. 8). This detrending removes the contributions to the standard deviation that do not reflect fluctuations in the dynamics. One can see that the good agreement with the experimental matrix is found in a region of the parameter space that presents some level of synchronization (panel a) and fluctuations (panel b). These dynamical conditions allow for the emergence of synchronization on the functional networks and also keep some level of flexibility for the emergence of different synchronized patterns over time. Figure 9c, d further corroborates this balance in the simulated, metastable dynamics. The values  $C = 54$  and  $v = 5$  m/s, which lead the maximum Pearson correlation between simulated and experimental functional connectivities, are marked by white circles and a blue star. These findings are consistent with the previous simulations of task-free (Cabral et al. 2011, 2014) and task-dependent (Hellyer et al. 2014) brain activity, which are based on similar simplified models that take into account a few key parameters of structural and functional brain connectivity.

The experimental fMRI data sets used in this paper are available from the *1000 Functional Connectome Project* Web site ([http://fcon\\_1000.projects.nitrc.org/](http://fcon_1000.projects.nitrc.org/)). We consider functional scans from the Berlin Margulies data to calculate the group average. The data consist of open-eyed resting-state measurements of 26 subjects (ages 23–44) (Biswal 2010). For details on the preprocessing steps, see Vuksanović and Hövel (2014). For the anatomical connectivity probability, we use DW-MRI data from a study described in Iturria-Medina et al. (2008).

## 5 Conclusions

Modern brain imaging methods allow for a quantitative study of both local activity dynamics and the interdependence between activities in anatomically distant cortical areas, which is known as functional connectivity. With this review, we have summarized one of many multidisciplinary approaches to model such functional interactions. Leveraging interdisciplinary theoretical techniques, inspired by complex system theory and applied mathematics, and existing experimental data from noninvasive brain imaging, the proposed modeling framework contributes to the development of viable analytical and modeling techniques leading to significant insight into dynamical mechanisms of the brain.

The particular model, which we consider in this review, combines experimental anatomical and functional connectivity between cortical regions to generate a network topology of the brain at rest. By varying the network interactions (using different coupling strengths and signal transmission velocities), it is possible to obtain correlation patterns in the simulated BOLD fMRI time series that are in agreement with experiments. We have shown that the model leads to the best agreement for a dynamical state that exhibits a balance between synchrony and temporal variations in synchrony. The proposed model allows to investigate the role of network structure and in particular indirect connections between distant cortical regions and to explore functional connectivity in the brain using numerical simulations of delay-coupled phase oscillators. For example, we have found higher functional connectivity, if the neighborhoods of respective nodes show a greater overlap. We have also compared the influence of time delay

considering fiber track lengths and Euclidean distances between brain regions. We have observed no qualitative difference in the simulations. This means that Euclidean distances—after rescaling—may be used to account for realistic coupling delays.

The procedure can easily be extended to a much larger field of brain states. For example, one can alter the adjacency matrix of the task-negative system by increasing the weights of connections between task-related nodes above unity, simulating a greater statistical relevance within the task-evoked state. Additionally, this procedure might give some insight into the brain shifting from the resting-state to task-evoked states and back.

The flexibility of the network topology generating process also gives an opportunity to manipulate node connections to adapt to neural activity observed in fMRI measurements of patients suffering from various brain disorders. Indeed, similar data-driven models had contributed to understanding some mechanisms of brain disorders (Demirtas and Deco 2018; Hutchings et al. 2015; Deco and Kringelbach 2014; Cabral et al. 2012).

The limitation of this model is given by its purpose, which was to provide explanations for mechanisms generating coordinated activity between spatially distant brain regions. We focus our computations on how these long-distance correlations arise from realistic functional interactions, i.e., those that are also supported by direct structural connections. Thus, our model does not consider the role of coupling topologies that correspond directly to structural connectivity data. Models based on these structural connectivity topologies have been explored extensively in several studies (see Cabral et al. 2011; Hellyer et al. 2014; Cabral et al. 2012), reaching—similarly to our model—an agreement with the experimental data only to a certain extent.

The model presented in this paper does not strive to give an accurate representation of the physiologically realistic brain activity. A much more physiology-based approach is needed to achieve a full understanding of the relation between experimental fMRI data and simulated neural activity. However, this goes beyond the scope of the main focus of the present work that discusses a specific approach to find a simple way to simulate neural time series and to transform them into data, which can be compared to experimental fMRI measurements. This simplification is also adopted in similar studies found in Cabral et al. (2011, 2012, 2014) and Deco and Jirsa (2012). The model that we presented in this review can be extended in various way to incorporate more physiological details such as heterogeneities in the signal transmission velocities accounting for myelination or axon thickness. In addition, link weights can be introduced in the coupling matrix to include more information from experimental data.

The studies summarized in this article contribute to a better understanding of the relationship between complex brain networks and temporal dynamics of brain activity. They might also serve as a starting point to investigate brain network reconfigurations providing a modeling framework to explore transient, dynamical interactions, which enable diverse cognitive functions.

**Acknowledgements** AV and PH acknowledge support by Deutsche Forschungsgemeinschaft under Grant No. HO4695/3-1 and within the framework of Collaborative Research Center 910. We thank Yasser Iturria-Medina for sharing the DW-MRI data including fiber lengths used in the study. We also thank Jason Bassett for helpful discussions.

## A List of Cortical and Subcortical Regions

See Table 1.

**Table 1** Cortical and subcortical regions according to the Automated Anatomical Labeling (AAL) template image (Tzourio-Mazoyer et al. 2002)

Index R/L	Anatomical description	Label
1/46	Precentral	PRE
2/47	Frontal sup	F1
3/48	Frontal sup orb	F10
4/49	Frontal mid	F2
5/50	Frontal mid orb	F20
6/51	Frontal inf oper	F30P
7/52	Frontal inf tri	F3T
8/53	Frontal inf orb	F30
9/54	Rolandic oper	RO
10/55	Supp motor area	SMA
11/56	Olfactory	OC
12/57	Frontal sup medial	F1M
13/58	Frontal mid orb	SMG
14/59	Gyrus rectus	GR
15/60	Insula	IN
16/61	Cingulum ant	ACIN
17/62	Cingulum mid	MCIN
18/63	Cingulum post	PCIN
19/64	Hippocampus	HIP
20/65	ParaHippocampal	PHIP
21/66	Amygdala	AMYG
22/67	Calcarine	V1
23/68	Cuneus	Q
24/69	Lingual	LING
25/70	Occipital sup	O1
26/71	Occipital mid	O2
27/72	Occipital inf	O3
28/73	Fusiform	FUSI
29/74	Postcentral	POST
30/75	Parietal sup	P1
31/76	Parietal inf	P2
32/77	Supramarginal gyrus	SMG
33/78	Angular	AG
34/79	Precuneus	PQ
35/80	Paracentral lobule	PCL
36/81	Caudate	CAM
37/82	Putamen	PUT
38/83	Pallidum	PAL

**Table 1** continued

Index R/L	Anatomical description	Label
39/84	Thalamus	THA
40/85	Heschi	HES
41/86	Temporal sup	T1
42/87	Temporal pole sup	T1P
43/88	Temporal mid	T2
44/89	Temporal pole mid	T2P
45/90	Temporal inf	T3

Indexes from 1–45 and 46–90 indicate right (R) and left (L) hemisphere respectively, and refer to the order in which the brain regions of interest are arranged in all connectivity, adjacency, and distance matrices of this paper

## References

- Acebrón, J.A., Bonilla, L.L., Pérez Vicente, C.J., Ritort, F., Spigler, R.: The Kuramoto model: a simple paradigm for synchronization phenomena. *Rev. Mod. Phys.* **77**, 137 (2005)
- Arenas, A., Díaz-Guilera, A., Pérez Vicente, C.J.: Synchronization reveals topological scales in complex networks. *Phys. Rev. Lett.* **96**, 114102 (2006)
- Balanov, A.G., Janson, N.B., Postnov, D.E., Sosnovtseva, O.V.: *Synchronization: From Simple to Complex*. Springer, Berlin (2009)
- Barttfeld, P., Uhrig, L., Sitt, J.D., Sigman, M., Jarraya, B., Dehaene, S.: Signature of consciousness in the dynamics of resting-state brain activity. *Proc. Natl. Acad. Sci. USA* **112**, 887 (2015)
- Bergner, A., Frasca, M., Sciuto, G., Buscarino, A., Ngamga, E.J., Fortuna, L., Kurths, J.: Remote synchronization in star networks. *Phys. Rev. E* **85**, 026208 (2012)
- Biswal, B.B.: Toward discovery science of human brain function. *Proc. Natl. Acad. Sci. USA* **107**, 4734 (2010)
- Biswal, B., Yetkin, F.Z., Haughton, V.M., Hyde, J.S.: Functional connectivity in the motor cortex of resting human brain using echo-planar MRI. *Magn. Reson. Med.* **34**, 537 (1995)
- Boccaletti, S., Kurths, J., Osipov, G., Valladares, D.L., Zhou, C.S.: The synchronization of chaotic systems. *Phys. Rep.* **366**, 1 (2002)
- Bola, M., Sabel, B.A.: Dynamic reorganization of brain functional networks during cognition. *NeuroImage* **114**, 398 (2015)
- Breakspear, M., Roberts, J.A., Terry, J.R., Rodrigues, S., Mahant, N., Robinson, P.A.: A unifying explanation of primary generalized seizures through nonlinear brain modeling and bifurcation analysis. *Cereb. Cortex* **16**, 1296 (2006)
- Breakspear, M., Heitmann, S., Daffertshofer, A.: Generative models of cortical oscillations: neurobiological implications of the Kuramoto model. *Front. Hum. Neurosci.* **4**, 190 (2010)
- Bressler, S.L., Menon, V.: Large-scale brain networks in cognition: emerging methods and principles. *Trends Cogn. Sci.* **14**, 277 (2010)
- Bullmore, E.T., Bassett, D.S.: Brain graphs: graphical models of the human brain connectome. *Annu. Rev. Clin. Psychol.* **7**, 113 (2011)
- Bullmore, E.T., Sporns, O.: Complex brain networks: graph theoretical analysis of structural and functional systems. *Nat. Rev. Neurosci.* **10**, 186 (2009)
- Cabral, J., Hugues, E., Sporns, O., Deco, G.: Role of local network oscillations in resting-state functional connectivity. *Neuroimage* **57**, 130 (2011)
- Cabral, J., Hugues, E., Kringelbach, M.L., Deco, G.: Modeling the outcome of structural disconnection on resting-state functional connectivity. *Neuroimage* **62**, 1342 (2012)
- Cabral, J., Fernandes, H.M., Van Hartevelt, T.J., James, A.C., Kringelbach, M.L.: Structural connectivity in schizophrenia and its impact on the dynamics of spontaneous functional networks. *Chaos* **23**, 046111 (2013)


- Cabral, J., Luckhoo, H., Woolrich, M.W., Joensson, M., Mohseni, H., Baker, A., Kringelbach, M.L., Deco, G.: Exploring mechanisms of spontaneous functional connectivity in MEG: how delayed network interactions lead to structured amplitude envelopes of band-pass filtered oscillations. *Neuroimage* **90**, 423 (2014a)
- Cabral, J., Kringelbach, M.L., Deco, G.: Exploring the network dynamics underlying brain activity during rest. *Prog. Neurobiol.* **114**, 102 (2014b)
- Carhart-Harris, R., Muthukumaraswamy, S., Roseman, L., Kaelen, M., Droog, W., Murphy, K., Tagliazucchi, E., Schenberg, E.E., Nest, T., Orban, C., Leech, R., Williams, L.T., Williams, T.M., Bolstridge, M., Sessa, B., McGonigle, J., Sereno, M.I., Nichols, D., Hellyer, P.J., Hobden, P., Evans, J., Singh, K.D., Wise, R.G., Curran, H.V., Feilding, A., Nutt, D.J.: Neural correlates of the LSD experience revealed by multimodal neuroimaging. *Proc. Natl. Acad. Sci. USA* **113**, 4853 (2016)
- Ciccarelli, O., Catani, M., Johansen-Berg, H., Clark, C., Thompson, A.: Diffusion-based tractography in neurological disorders: concepts, applications, and future developments. *Lancet Neurol.* **7**, 715 (2008)
- Clayden, J.D.: Imaging connectivity: MRI and the structural networks of the brain. *Funct. Neurol.* **28**, 197 (2013)
- Cole, D.M., Smith, S.M., Beckmann, C.F.: Advances and pitfalls in the analysis and interpretation of resting-state fMRI data. *Front. Syst. Neurosci.* **4**, 8 (2010)
- Damoiseaux, J.S., Rombouts, S.A.R.B., Barkhof, F., Scheltens, P., Stam, C.J., Smith, S.M., Beckmann, C.F.: Consistent resting-state networks across healthy subjects. *Proc. Natl. Acad. Sci. USA* **103**, 13848 (2006)
- Dang-Vu, T.T., Schabus, M., Desseilles, M., Albouy, G., Boly, M., Darsaud, A., Gais, S., Rauchs, G., Sterpenich, V., Vandewalle, G., Carrier, J., Moonen, G., Balteau, E., Degueldre, C., Luxen, A., Phillips, C., Maquet, P.: Spontaneous neural activity during human slow wave sleep. *Proc. Natl. Acad. Sci. USA* **105**, 15160 (2008)
- Deco, G., Jirsa, V.K.: Ongoing cortical activity at rest: criticality, multistability, and ghost attractors. *J. Neurosci.* **32**, 3366 (2012)
- Deco, G., Kringelbach, M.L.: Great expectations: using whole-brain computational connectomics for understanding neuropsychiatric disorders. *Neuron* **84**, 892 (2014)
- Deco, G., Jirsa, V.K., McIntosh, A.R.: Emerging concepts for the dynamical organization of resting-state activity in the brain. *Nat. Rev. Neurosci.* **12**, 43 (2011)
- Deco, G., Jirsa, V.K., McIntosh, A.R.: Resting brains never rest: computational insights into potential cognitive architectures. *Trends Neurosci.* **36**, 268 (2013)
- Demirtas, M., Deco, G.: Chapter 4—computational models of dysconnectivity in large-scale resting-state networks. In: Anticevic, A., Murray, J.D. (eds.) *Computational Psychiatry*, pp. 87–116. Academic Press, New York (2018)
- Desjardins, A.E., Kiehl, K.A., Liddle, P.F.: Removal of confounding effects of global signal in functional MRI analyses. *NeuroImage* **13**, 751 (2001)
- Farooq, H., Xu, J., Nam, J.W., Keefe, D.F., Yacoub, E., Georgiou, T., Lenglet, C.: Microstructure imaging of crossing (MIX) white matter fibers from diffusion MRI. *Sci. Rep.* **6**, 38927 (2016)
- Felleman, D.J., Van Essen, D.C.: Distributed hierarchical processing in the primate cerebral cortex. *Cereb. Cortex* **1**, 1 (1991)
- FitzHugh, R.: Impulses and physiological states in theoretical models of nerve membrane. *Biophys. J.* **1**, 445 (1961)
- Friston, K., Dolan, R.J.: Computational and dynamic models in neuroimaging. *NeuroImage* **52**, 752 (2010)
- Friston, K., Mechelli, A., Turner, R., Price, C.J.: Nonlinear responses in fMRI: the balloon model, Volterra kernels, and other hemodynamics. *NeuroImage* **12**, 466 (2000)
- Greve, D.N., Brown, G.G., Mueller, B.A., Glover, G., Liu, T.T.: A survey of the sources of noise in fMRI. *Psychometrika* **78**, 396 (2013)
- Hauptmann, C., Omel'chenko, O.E., Popovych, O., Maistrenko, Y., Tass, P.: Control of spatially patterned synchrony with multisite delayed feedback. *Phys. Rev. E* **76**, 066209 (2007)
- Haynes, J.D., Rees, G.: Decoding mental states from brain activity in humans. *Nat. Rev. Neurosci.* **7**, 523 (2006)
- Heeger, D.J., Ress, D.: What does MRI tell us about neuronal activity? *Nat. Rev. Neurosci.* **3**, 142 (2002)
- Hellyer, P.J., Shanahan, M., Scott, G., Wise, R.J.S., Sharp, D.J., Leech, R.: The control of global brain dynamics: opposing actions of frontoparietal control and default mode networks on attention. *J. Neurosci.* **34**, 451 (2014)

- Hodgkin, A.L., Huxley, A.F.: A quantitative description of membrane current and its application to conduction and excitation in nerve. *J. Physiol.* **117**, 500 (1952)
- Honey, C.J., Sporns, O., Cammoun, L., Gigandet, X., Thiran, J.P., Meuli, R., Hagmann, P.: Predicting human resting-state functional connectivity from structural connectivity. *Proc. Natl. Acad. Sci. USA* **106**, 2035 (2009)
- Huang, Z., Dai, R., Wu, X., Yang, Z., Liu, D., Hu, J., Gao, L., Tang, W., Mao, Y., Jin, Y., Wu, X., Liu, B., Zhang, Y., Lu, L., Laureys, S., Weng, X., Northoff, G.: The self and its resting state in consciousness: an investigation of the vegetative state. *Hum. Brain Mapp.* **35**, 1997 (2014)
- Hutchings, F., Han, C.E., Keller, S.S., Weber, B., Taylor, P.N., Kaiser, M.: Predicting surgery targets in temporal lobe epilepsy through structural connectome based simulations. *PLoS Comput. Biol.* **11**, e1004642 (2015)
- Iturria-Medina, Y., Sotero, R.C., Canales-Rodríguez, E.J., Alemán-Gómez, Y., Melie-García, L.: Studying the human brain anatomical network via diffusion-weighted MRI and graph theory. *NeuroImage* **40**, 1064 (2008)
- Izhikevich, E.M.: Which model to use for cortical spiking neurons? *IEEE Trans. Neural Netw.* **15**, 1063 (2004)
- Jbabdi, S., Sotiropoulos, S.N., Haber, S.N., Van Essen, D.C., Behrens, T.E.: Measuring macroscopic brain connections in vivo. *Nat. Neurosci.* **18**, 1546 (2015)
- Jirsa, V.K., Haken, H.: Field theory of electromagnetic brain activity. *Phys. Rev. Lett.* **77**, 960 (1996)
- Kanwisher, N.: Functional specificity in the human brain: a window into the functional architecture of the mind. *Proc. Natl. Acad. Sci. USA* **107**, 11163 (2010)
- Keane, A., Dahms, T., Lehnert, J., Suryanarayana, S.A., Hövel, P., Schöll, E.: Synchronisation in networks of delay-coupled type-I excitable systems. *Eur. Phys. J. B* **85**, 407 (2012)
- Koch, M.A., Norris, D.G., Hund-Georgiadis, M.: An investigation of functional and anatomical connectivity using magnetic resonance imaging. *NeuroImage* **16**, 241 (2002)
- Kruggel, F., von Cramon, D.Y., Descombes, X.: Comparison of filtering methods for fMRI datasets. *NeuroImage* **10**, 530 (1999)
- Kuramoto, Y.: Self-entrainment of a population of coupled non-linear oscillators. In: Araki, H. (ed.) *International Symposium on Mathematical Problems in Theoretical Physics*, vol. 39 of *Lecture Notes in Physics*, pp. 420–422. Springer, Berlin (1975)
- Lehnert, J., Dahms, T., Hövel, P., Schöll, E.: Loss of synchronization in complex neural networks with delay. *Europhys. Lett.* **96**, 60013 (2011)
- Liang, X., Tang, M., Dhamala, M., Liu, Z.: Phase synchronization of inhibitory bursting neurons induced by distributed time delays in chemical coupling. *Phys. Rev. E* **80**, 066202 (2009)
- Liu, Y., Liang, M., Zhou, Y., He, Y., Hao, Y., Song, M., Yu, C., Liu, H., Liu, Z., Jiang, T.: Disrupted small-world networks in schizophrenia. *Brain* **131**, 945 (2008)
- Lowe, M.J.: A historical perspective on the evolution of resting-state functional connectivity with MRI. *Magn. Reson. Mater. Phys.* **23**, 279 (2010)
- Masoller, C., Torrent, M.C., García-Ojalvo, J.: Interplay of subthreshold activity, time-delayed feedback, and noise on neuronal firing patterns. *Phys. Rev. E* **78**, 041907 (2008)
- Masoller, C., Torrent, M.C., García-Ojalvo, J.: Dynamics of globally delay-coupled neurons displaying subthreshold oscillations. *Phil. Trans. R. Soc. A Math. Phys. Eng. Sci.* **367**, 3255 (2009)
- Mosekilde, E., Maistrenko, Y., Postnov, D.: *Chaotic Synchronization: Applications to Living Systems*. World Scientific, Singapore (2002)
- Muldoon, S.F., Pasqualetti, F., Gu, S., Cieslak, M., Grafton, S.T., Vettel, J.M., Bassett, D.S.: Stimulation-based control of dynamic brain networks. *PLoS Comput. Biol.* **12**, e1005076 (2016)
- Nagumo, J., Arimoto, S., Yoshizawa, S.: An active pulse transmission line simulating nerve axon. *Proc. IRE* **50**, 2061 (1962)
- Nicosia, V., Valencia, M., Chavez, M., Díaz-Guilera, A., Latora, V.: Remote synchronization reveals network symmetries and functional modules. *Phys. Rev. Lett.* **110**, 174102 (2013)
- Noirhomme, Q., Soddu, A., Lehembre, R., Vanhauzenhuyse, A., Boveroux, P., Boly, M., Laureys, S.: Brain connectivity in pathological and pharmacological coma. *Front. Syst. Neurosci.* **4**, 160 (2010)
- Onias, H., Viol, A., Palhano-Fontes, F., Andrade, K.C., Sturzbecher, M., Viswanathan, G.M., de Araujo, D.B.: Brain complex network analysis by means of resting state fMRI and graph analysis: will it be helpful in clinical epilepsy? *Epilepsy Behav.* **38**, 71 (2014)
- Pikovsky, A., Rosenblum, M.G., Kurths, J.: *Synchronization: A Universal Concept in Nonlinear Sciences*. Cambridge University Press, Cambridge (2001)

- Popovych, O., Yanchuk, S., Tass, P.: Delay- and coupling-induced firing patterns in oscillatory neural loops. *Phys. Rev. Lett.* **107**, 228102 (2011)
- Power, J.D., Mitra, A., Laumann, T.O., Snyder, A.Z., Schlaggar, B.L., Petersen, S.E.: Methods to detect, characterize, and remove motion artifact in resting state fMRI. *Neuroimage* **84**, 320 (2014)
- Rodrigues, F.A., Peron, T.K.D.M., Ji, P., Kurths, J.: The Kuramoto model in complex networks. *Phys. Rep.* **610**, 1 (2016)
- Rossoni, E., Chen, Y., Ding, M., Feng, J.: Stability of synchronous oscillations in a system of Hodgkin–Huxley neurons with delayed diffusive and pulsed coupling. *Phys. Rev. E* **71**, 061904 (2005)
- Rubinov, M., Sporns, O.: Complex network measures of brain connectivity: uses and interpretations. *Neuroimage* **52**, 1059 (2010)
- Rubinov, M., Knock, S.A., Stam, C.J., Micheloyannis, S., Harris, A.W.F., Williams, L.M., Breakspear, M.: Small-world properties of nonlinear brain activity in schizophrenia. *Hum. Brain Mapp.* **30**, 403 (2009)
- Rudie, J.D., Brown, J.A., Beck-Pancer, D., Hernandez, L.M., Dennis, E.L., Thompson, P.M., Bookheimer, S.Y., Dapretto, M.: Altered functional and structural brain network organization in autism. *NeuroImage Clin.* **2**, 79 (2013)
- Sanz-Leon, P., Knock, S.A., Spiegler, A., Jirsa, V.K.: Mathematical framework for large-scale brain network modeling in The Virtual Brain. *Neuroimage* **111**, 385 (2015)
- Schall, J.D.: On building a bridge between brain and behavior. *Annu. Rev. Psychol.* **55**, 23 (2004)
- Schrouff, J., Perlberg, V., Boly, M., Marrelec, G., Boveroux, P., Vanhaudenhuyse, A., Bruno, M.A., Laureys, S., Phillips, C., Péligrini-Issac, M., Maquet, P., Benali, H.: Brain functional integration decreases during propofol-induced loss of consciousness. *NeuroImage* **57**, 198 (2011)
- Senthilkumar, D.V., Kurths, J., Lakshmanan, M.: Inverse synchronizations in coupled time-delay systems with inhibitory coupling. *Chaos* **19**, 023107 (2009)
- Seth, A.K., Chorley, P., Barnett, L.C.: Granger causality analysis of fMRI BOLD signals is invariant to hemodynamic convolution but not downsampling. *NeuroImage* **65**, 540 (2013)
- Shanahan, M.: Metastable chimera states in community-structured oscillator networks. *Chaos* **20**, 013108 (2010)
- Sporns, O.: *Networks of the Brain*. MIT Press, Cambridge (2011)
- Sporns, O.: Structure and function of complex brain networks. *Dialog. Clin. Neurosci.* **15**, 247 (2013)
- Sporns, O., Tononi, G., Kötter, R.: The human connectome: a structural description of the human brain. *PLoS Comput. Biol.* **1**, e42 (2005)
- Strogatz, S.H.: From Kuramoto to Crawford: exploring the onset of synchronization in populations of coupled oscillators. *Physica D* **143**, 1 (2000)
- Tagliazucchi, E., Carhart-Harris, R., Leech, R., Nutt, D., Chialvo, D.R.: Enhanced repertoire of brain dynamical states during the psychedelic experience. *Hum. Brain Mapp.* **35**, 5442 (2014)
- Talairach, J., Tournoux, P.: *Co-planar Stereotaxic Atlas of the Human Brain. 3-Dimensional Proportional System: An Approach to Cerebral Imaging*. Thieme, New York (1988)
- Tognoli, E., Kelso, J.A.S.: The metastable brain. *Neuron* **81**, 35 (2014)
- Tzourio-Mazoyer, N., Landeau, B., Papathanassiou, D., Crivello, F., Etard, O., Delcroix, N., Mazoyer, B., Joliot, M.: Automated anatomical labeling of activations in SPM using a macroscopic anatomical parcellation of the MNI MRI single-subject brain. *Neuroimage* **15**, 273 (2002)
- Uhlhaas, P., Pipa, G., Lima, B., Melloni, L., Neunschwander, S., Nikolic, D., Singer, W.: Neural synchrony in cortical networks: history, concept and current status. *Front. Integr. Neurosci.* **3**, 17 (2009)
- van den Heuvel, M.P., Hulshoff Pol, H.E.: Exploring the brain network: a review on resting-state fMRI functional connectivity. *Eur. Neuropsychopharmacol.* **20**, 519 (2010)
- Vása, F., Shanahan, M., Hellyer, P.J., Scott, G., Cabral, J., Leech, R.: Effects of lesions on synchrony and metastability in cortical networks. *NeuroImage* **118**, 456 (2015)
- Viol, A., Palhano-Fontes, F., Onias, H., de Araujo, D.B., Viswanathan, G.M.: Shannon entropy of brain functional complex networks under the influence of the psychedelic Ayahuasca. *Sci. Rep.* **7**, 7388 (2017)
- Vuksanović, V., Hövel, P.: Functional connectivity of distant cortical regions: role of remote synchronization and symmetry in interactions. *NeuroImage* **97**, 1 (2014)
- Vuksanović, V., Hövel, P.: Dynamic changes in network synchrony reveal resting-state functional networks. *Chaos* **25**, 023116 (2015)
- Vuksanović, V., Hövel, P.: Large-scale neural network model for functional networks of the human cortex. In: Pelster, A., Wunner, G. (eds.) *Selforganization in Complex Systems: The Past, Present, and Future*

- of Synergetics, Proceedings of the International Symposium, Hanse Institute of Advanced Studies Delmenhorst, pp. 345–352. Springer, Berlin (2016a). (Understanding Complex Systems)
- Vuksanović, V., Hövel, P.: Role of structural inhomogeneities in resting-state brain dynamics. *Cogn. Neurodyn.* **10**, 361 (2016b)
- Wang, Q.Y., Lu, Q.S.: Time delay-enhanced synchronization and regularization in two coupled chaotic neurons. *Chin. Phys. Lett.* **22**, 543 (2005)
- Wang, Q., Lu, Q., Chen, G.: Synchronization transition induced by synaptic delay in coupled fast-spiking neurons. *Int. J. Bifur. Chaos* **18**, 1189 (2008)
- Wang, Q., Lu, Q., Chen, G., Feng, Z., Duan, L.X.: Bifurcation and synchronization of synaptically coupled FHN models with time delay. *Chaos Solitons Fractals* **39**, 918 (2009)
- Wildie, M., Shanahan, M.: Hierarchical clustering identifies hub nodes in a model of resting-state brain activity. In: The 2012 International Joint Conference on Neural Networks (IJCNN), pp. 1–6. IEEE (2012)
- Womelsdorf, T., Schoffelen, J.M., Oostenveld, R., Singer, W., Desimone, R.: Modulation of neuronal interactions through neuronal synchronization. *Science* **316**, 1609 (2007)
- Xia, M., Wang, J., He, Y.: Brainnet viewer: a network visualization tool for human brain connectomics. *PLoS ONE* **8**, 1 (2013)

## Affiliations

Philipp Hövel<sup>1,2,3</sup>  · Aline Viol<sup>2,3</sup> · Philipp Loske<sup>2,4</sup> · Leon Merfort<sup>2</sup> · Vesna Vuksanović<sup>4</sup>

- ✉ Philipp Hövel  
phoevel@physik.tu-berlin.de
- Aline Viol  
aline.viol@bccn-berlin.de
- Vesna Vuksanović  
vesna.vuksanovic@abdn.ac.uk

- <sup>1</sup> School of Mathematical Sciences, University College Cork, Cork T12 XF62, Ireland
- <sup>2</sup> Institute of Theoretical Physics, Technische Universität Berlin, Hardenbergstraße 36, 10623 Berlin, Germany
- <sup>3</sup> Bernstein Center for Computational Neuroscience Berlin, Humboldt-Universität zu Berlin, Philippstraße 13, 10115 Berlin, Germany
- <sup>4</sup> Aberdeen Biomedical Imaging Centre, University of Aberdeen, Lilan Sutton Building, Foresterhill, Aberdeen AB25 2ZD, UK